Nanoscale Metal Oxide Particles as Chemical Reagents. Intrinsic Effects of Particle Size on Hydroxyl Content and on Reactivity and Acid/Base Properties of Ultrafine Magnesium Oxide

Hidenobu Itoh, Suchada Utamapanya, Jane V. Stark, Kenneth J. Klabunde,* and John R. Schlup

Departments of Chemistry and Chemical Engineering, Kansas State University, Manhattan, Kansas 66506

Received August 24, 1992. Revised Manuscript Received October 20, 1992

Two sizes of ultrafine magnesium oxide particles have been carefully compared for intrinsic surface chemistry differences. Ultrahigh surface area MgO (400-650 m^2/gm) prepared by an autoclave hypercritical drying (aerogel) procedure has been compared with conventionally prepared MgO (100-300 m^2/gm) for hydroxyl surface concentration (also residual OCH_3), pyridine, benzene, xylene, and nitrobenzene adsorption. The aerogel-prepared material exhibited the highest surface area (650 m^2/g) after a 300 °C heat treatment, while the conventional sample's surface area went up to 300 m^2/g after a 400 °C treatment. Both FT-IR/photoacoustic and conventional transmission IR spectroscopies were employed to monitor the adsorbed species. Amounts of material adsorbed were also quantitatively determined. Careful comparisons between the smaller and larger particle MgO were made. It was shown that surface –OH concentrations were similar but that the larger particles allowed more geminal pair reactions of –OH with $AlEt_3$ to yield $EtAl-(O_2)(ad)$ rather than $Et_2Al-O(ad)$. It was also found that the MgO particles adsorbed pyridine on the Mg^{2+} sites and not the Bronsted sites. However, benzene did adsorb on Bronsted sites, and IR shifts showed that the smaller particles exhibited weaker Bronsted acidity. Nitrobenzene adsorption suggested weaker Lewis basicity as well. It is proposed that basic/reducing character depends more on domains and is encouraged by larger particle size and Bronsted acidity is also encouraged by –OH surface island domains. Overall, the results show that particle size can have intrinsic effects on surface chemistry.

Introduction

As interest in the chemistry and physical properties of nanoscale particles (clusters) continues to grow, it becomes important to determine if and how size alone causes intrinsic differences. It has been demonstrated that optical, magnetic, and melting points are affected by particle size.[1] However, would surface chemistry be intrinsically different due to size alone? This is a question we have attempted to answer by a careful study of two well-characterized samples, which we report herein. The nanoscale particles we chose are of MgO, one of 4-nm and the other of 9-nm average crystallite sizes.

Magnesium oxide is a unique solid because of its highly ionic character, simple stoichiometry, and crystal structure and because it can be prepared in widely variable particle sizes.[2-12] We have reported earlier on preparative methods for nanoscale particles of MgO and have improved and standardized these methods so that reproducibility is excellent and particle size distribution is relatively narrow.

To probe for intrinsic surface chemistry differences for these 4-nm vs 9-nm MgO particles, a variety of surface probes are available. These include catalysis,[6,7] detection of defect sites,[4,5] molecular adsorbates,[13,14] and photoluminescence.[6,7,15]

Pyridine has been used as an extant probe of surface acidity.[16-20] It has been found to interact with ionic metal oxides by three different modes. The first involves transfer of a proton from a surface hydroxyl to form a pyridinium ion. The second involves coordination of the nitrogen lone

---

* To whom correspondence should be addressed at the Department of Chemistry.

(1) Andres, R. P.; Averback, R. S.; Brown, W. L.; Brus, L. E.; Goddard, W. A.; Kaldor, A.; Louis, S. G.; Moskovits, M.; Peercy, P. S.; Riley, S. J.; Siegel, R. W.; Spaepan, F.; Wang, Y. *J. Mater. Res.* 1989, *4*, 704.

(2) Tanabe, K. *Solid Acids and Bases*; Academic Press: New York, 1970.

(3) Nieves, I.; Klabunde, K. J. *Mater. Chem. Phys.* 1988, *18*, 485.

(4) Hughes, A. E.; Henderson, B. In *Point Defects in Solids*; Crawford, J. H., Jr., Slifkin, L. M., Eds.; Plenum Press: New York, 1972; Vol. 1, p 381.

(5) Morris, R. M. Ph.D. Thesis, University of North Dakota, Grand Forks, North Dakota, 1981.

(6) Che, M. In *Adsorption and Catalysis on Oxide Surfaces*; (Che M., Bond, G. C., Eds.;) Elsevier Science: Amsterdam, 1985; p 11.

(7) Coluccia, S. In *Adsorption and Catalysis on Oxide Surfaces*; Che, M., Bond, G. C., Eds.; Elsevier Science: Amsterdam, 1985; p 59.

(8) Zecchina, A.; Coluccia, S.; Morterra, C. *Appl. Spectrosc. Rev.* **1985**, *21*, 259.

(9) Utamapanya, S.; Klabunde, K. J.; Schlup, J. *Chem. Mater.* **1991**, *3*, 175.

(10) Atteya, M.; Klabunde, K. J. *Chem. Mater.* **1991**, *3*, 183.

(11) Li, Y. X.; Klabunde, K. J. *Langmuir* **1991**, *7*, 1388.

(12) Li, Y. X.; Schlup, J.; Klabunde, K. J. *Langmuir* **1991**, *7*, 1394.

(13) Garrone, E.; Stone, F. S. *J. Chem. Soc., Faraday Trans. 1* **1987**, *83*, 1237.

(14) Ito, T.; Watanabe, T.; Tashiro, T.; Toi, K. *J. Chem. Soc., Faraday Trans. 1* 1989, 2381.

(15) Anpo, M.; Yamada, Y.; Kubokawa, Y.; Coluccia, S.; Zecchina, A.; Che, M. *J. Chem. Soc., Faraday Trans. 1* **1988**, *84*, 751.

(16) Austermann, R. L.; Denley, D. R.; Hart, D. W.; Himelfarb, P. B.; Irwin, R. M.; Narayana, M.; Szentirmay, R.; Tang, S. C.; Yeates, R. C. *Anal. Chem.* **1987**, *59*, 68R.

(17) Boehm, H.-P.; Knozinger, H. In *Catalysis*; Anderson, J. R., Boudart, M., Eds.; Springer-Verlag: Berlin, 1983; p 39.

(18) Kung, M. C.; Kung, H. H. *Catal. Rev. Sci. Eng.* **1985**, *27*, 425.

(19) Verdrine, J. C. In *Surface Properties and Catalysis by Non-Metals*; Bonnelle, J. P., Delmon, B., Derouane, E., Ed.; D. Reidel: Dordrecht, 1963; p 123.

(20) Yates, J. T., Jr., Madey, T. E., Eds. *Vibrational Spectroscopy of Molecules on Surfaces*; Plenum Press: New York, 1987.

0897-4756/93/2805-0071$04.00/0

pair with a Lewis acid site (metal ion, LPy bonding mode). The third, and weakest interaction is through hydrogen bonding to a surface –OH group. Infrared spectroscopy has been a powerful tool for differentiating among these three modes as well as measuring the relative interaction strength.[18,19,21]

Indeed, IR has been a powerful probe of other adsorbed species.[8,17-30] and we have used it in this study for monitoring adsorption of benzene, xylene, nitrobenzene, and pyridine.

Finally, when considering the surface chemistry of ionic metal oxides, it is clear that surface –OH groups are of paramount importance.[31] Surface reactivity is a strong function of prior heat treatment procedures, and this in turn affects surface –OH concentrations. Unfortunately, careful, analytical determinations of surface –OH concentrations are difficult to carry out and therefore are not commonly found in the literature, and this hampers valid interpretation of catalytic and spectroscopic results. Herein, we report detailed studies of surface –OH concentrations and also have determined what fraction of –OH groups are in an orientation favorable to react as double ensembles.

In this report all of these spectroscopic probes and experimental approaches have been focused on the question of whether particle size variance in the nanometer-size range affects surface chemistry.

Experimental Setup

(A) Preparation of Samples. The preparation of CP-MgO and AP-MgO have been described earlier.[9] The final heat treatment to the desired temperature was carried out under dynamic vacuum.

(B) Adsorption Procedure. *(1) FT-IR/PAS Studies.* The adsorption of probe molecules was carried out at room temperature. Initially the vacuum above the sample was less than 3×10^{-3} Torr. The vapor of dry, degassed pyridine or nitrobenzene was exposed to the sample for a desired period of time. Then the sample was isolated from the organic liquid reservoir and transferred to the PA cell (MTEC Model 100) under a N_2 atmosphere.

In cases where it was desired that physisorbed organic molecules were to be removed, before transfer to the PA cell the sample was cryogenically evacuated for 10 min at room temperature. Spectra were recorded on a Mattson-Cygnus 100 FT-IR.

(2) Transmission IR Studies. The magnesium hydroxide samples (ca. 10 mg) were pressed into pellets (12- or 20-mm diameter) and treated at the desired temperature in the lower section of an in situ IR cell[35] for 2 h. The pellet was then moved to the IR window section, and treated with the desired chemicals as described below:

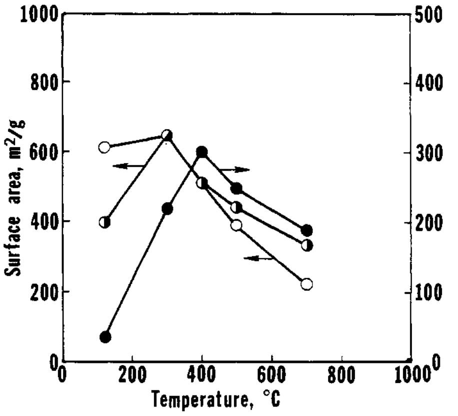

Figure 1. Surface areas as a function of heat treatment/evacuation temperature. (○) AP-MgO-a; (○) AP-MgO-b (aged); (●) CP-MgO.

After heat treatment, the sample was exposed to pyridine vapor (3 Torr) at room temperature for 10 min. The IR spectrum was measured after evacuation at room temperature or at 100 °C for 40 min so as to remove physisorbed species. Spectra were recorded on either a Perkin-Elmer 1330 infrared spectrometer or a high-resolution (±1 cm^{-1}) JEOL JIR-40X FT-IR.

Benzene and xylene adsorption: After heat treatment, the sample was exposed to benzene (80 Torr) or xylene vapor (8 Torr) at room temperature. The IR spectrum of the sample was measured with the adsorbate gas present as described above on the Perkin-Elmer instrument.

(3) Amounts of Adsorbed Material. A 0.2-g sample was placed in the basket of a spring balance and pretreated at 490 °C in vacuo. After heat treatment, the sample was exposed to pyridine vapor (3 Torr) at room temperature for 15 min, followed by evacuation at room temperature for 100 min. The difference of the spring length between initial and after adsorption was measured and compared to a calibration curve. Sensitivity of the balance is 0.1 mg.

(C) Measurement of Surface Hydroxyl Concentration by Reaction with Triethylaluminum, and Subsequent Reaction with Amyl Alcohol. A modified method of Sato and co-workers[32] was employed. A solution of $AlEt_3$ in pure, deoxygenated Decalin was prepared, and its concentration determined by using amyl alcohol titration.

Magnesium hydroxide samples were heat treated under vacuum at the desired temperature. The weight of the sample after heat treatment was calculated from the relationship between weight loss and heat treatment.

(D) Measurement of Surface Areas. Surface areas of the sample pretreated at various temperatures were measured from N_2 adsorption at liquid nitrogen temperature and applying the BET one-point method.

Results

(I) Particle Characterization. *(A) Surface Areas.* Surface areas were measured by BET methods. We were particularly interested in the effect of heat treatment (under vacuum). Figure 1 plots surface areas of two aerogel/autoclave prepared samples AP-MgO-a (freshly prepared) and AP-MgO-b (aged for 1 year after preparation) and conventionally (fresh) prepared CP-MgO-. In these notations AP signifies "aerogel/autoclave" prepared and these are the high surface area smaller particle size samples, and they start out with a significant amount of

---

(21) Kiselev, A. V.; Lygin, A. I. *Infrared Spectra of Surface Compounds*; Wiley: New York, 1975.

(22) Krishnan, K. *Appl. Spectrosc.* **1981**, *35*, 549.

(23) Rosencwaig, A. *Anal. Chem.* **1975**, *47*, 592A.

(24) Vidrine, D. W. In *Fourier Transform Infrared Spectroscopy*; Volume 3, Ferraro, J. R., Basile, L. J., Eds.; Academic Press: New York, 1982; p 125.

(25) Graham, J. A.; Grim, W. M., III; Fateley, W. G. In *Fourier Transform Infrared Spectroscopy*; Ferraro, J. R., Basile, L. J., Eds.; Academic Press: New York, 1981; Vol. 4, p 345.

(26) Riseman, S. M.; Massoth, F. E.; Dhar, G. M.; Eyring, E. M. *J. Phys. Chem.* **1982**, *86*, 1760.

(27) Hair, M. L. *Infrared Spectroscopy in Surface Chemistry*; Marcel Dekker: New York, 1967.

(28) Angell, C. L. In *Fourier Transform Infrared Spectroscopy*; Volume 3, Ferraro, J. R., Basile, L. J., Ed.; Academic Press: New York, 1982; p 1.

(29) Krishnan, K.; Ferraro, J. R. In *Fourier Transform Infrared Spectroscopy*; Ferraro, J. R., Basile, L. J., Eds.; Academic Press: New York, 1982; Vol. 3, p 149.

(30) Delgass, W. N.; Haller, G. L.; Kellerman, R.; Lunsford, J. H. *Spectroscopy in Heterogeneous Catalysis*; Academic Press: New York, 1979; Chapter 2.

(31) Hoq, M. F.; Nieves, I.; Klabunde, K. J. *J. Catal.*, **1990**, *123*, 349 and references therein.

(32) Sato, M.; Kanbayashi, T.; Kobayashi, N., Shima, Y. *J. Catal.* **1967**, *7*, 342.

Table I. Amount of Pyridine Adsorbed[a]

sample	pretreatment temp (°C)	surface area (m^2/g)	amt of Py (mol/g MgO, $\times 10^{-4}$)	adsorbed molecules/nm^2
AP-MgO	490	441	3.63	0.50
CP-MgO	490	248	2.93	0.71

[a] Measurements carried out at room temperature.

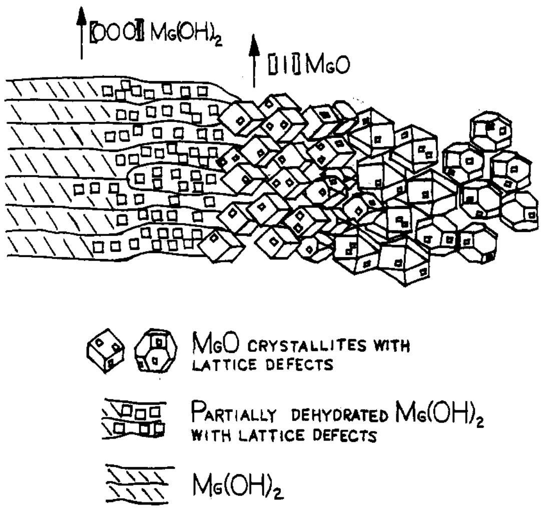

Figure 2. Evolution of nanoscale MgO crystallites from ultrafine $Mg(OH)_2$.

$Mg(OH)_2$ content, but with heating are dehydrated to MgO; CP signifies "conventionally prepared", and these are the lower surface area, larger particle samples.

Note the different axes on Figure 1. The CP-MgO sample started out at about 40 m^2/g but the surface area rose rather sharply upon heat treatment at 300 °C, and 400 °C brings it to about 300 m^2/g. Higher heat treatment temperature caused a decrease in surface area to around 200 m^2/g. In the case of the AP-MgO-a sample, the beginning surface area was very large, about 600 m^2/g and rose slightly upon 300 °C treatment, but higher temperature caused rather severe sintering to 400 m^2/g and eventually about 200 m^2/g. The AP-MgO-b sample started at 400 m^2/g, rose to over 600 m^2/g, and then fell to near 400 m^2/g with highest temperature treatment.

Weight loss as a function of temperature showed that both AP and CP samples dehydrated primarily in the 200–300 °C range. Further heating the CP sample to 400 °C maximized surface area by fully dehydrating the $Mg(OH)_2$. However, higher temperatures bring on the onset of particle sintering.

By employing 300 °C treatment AP-MgO samples of over 600 m^2/g could be prepared. It was apparent that conversion to ultrasmall MgO particles was facile for the AP samples, while a higher temperature was needed for the CP sample to reach maximum surface area. A likely explanation is that the CP samples were made up of larger $Mg(OH)_2$/MgO particles to start with and that complete dehydration was more difficult.

Examination of these samples by X-ray powder diffraction shows the clear progression of $Mg(OH)_2$/MgO conversion to pure MgO crystallites over the 200–300 °C range. Figure 2 attempts to illustrate how the $Mg(OH)_2 \rightarrow MgO$ conversion takes place such that surface area can *increase*. This phenomenon is important in the generation of nanoscale particles of MgO and is even more pronounced for CaO. In this process, as water is produced and desorbed, channels must form thereby isolating very small crystallites of the MgO or CaO being created. If the water vapor is removed quickly (vacuum or with a rapid flow of hot gas), steam-induced sintering is minimized, and these ultrafine particles survive.

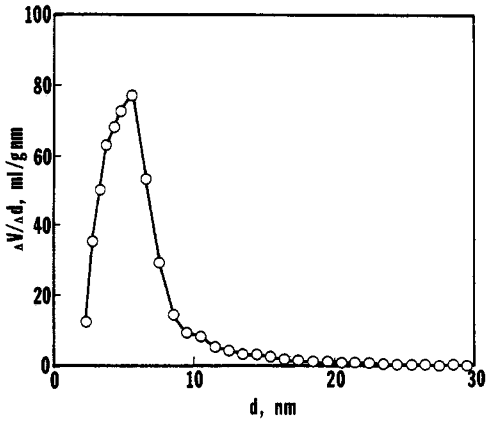

Figure 3. Pore volume distribution of AP-MgO heat treated/evacuated at 500 °C.

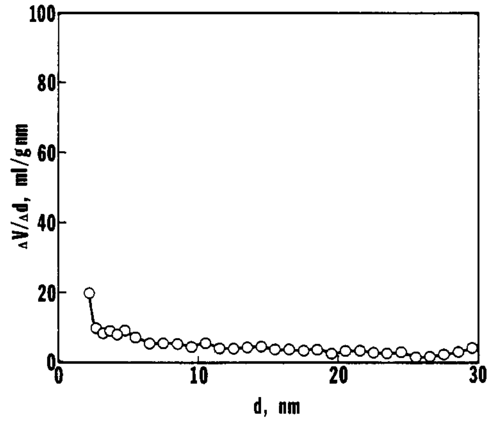

Figure 4. Pore volume distribution of CP-MgO heat treated/evacuated at 500 °C.

(*B*) *Pore Volumes.* Upon further examination of the nitrogen adsorption isotherms, plots of pore volume distributions were obtainable (Figures 3 and 4). The differences between the AP-MgO and CP-MgO samples are striking, the former exhibiting a sharp distribution from 2 to 9 nm with a maximum at about 6 nm. In the CP case, however, essentially no pore structure was detected.

(*C*) *Transmission Electron Microscopy.* The striking morphological differences between the AP and CP samples is clearly demonstrated by examination of TEM prints (Figure 5). The AP sample is make up of tiny individual spheroidal particles of about 1–5 nm that are weakly flocculated together. On the other hand, the CP-MgO sample is obviously much more crystalline, showing predominantly hexagonal platelet crystals. Idealized models of these crystallites have been drawn in Figure 6.

(*D*) *IR Studies.* Several differences between the AP and CP samples have been pointed out, among them lower temperature required to maximize surface area for the AP samples and more weight loss for the AP samples. Indeed, the observed weight loss for the AP samples was higher than the stoichiometric value for $Mg(OH)_2 \rightarrow MgO$, which should be 31%. We suspected that organic material must still be present from incomplete hydrolysis of the Mg-

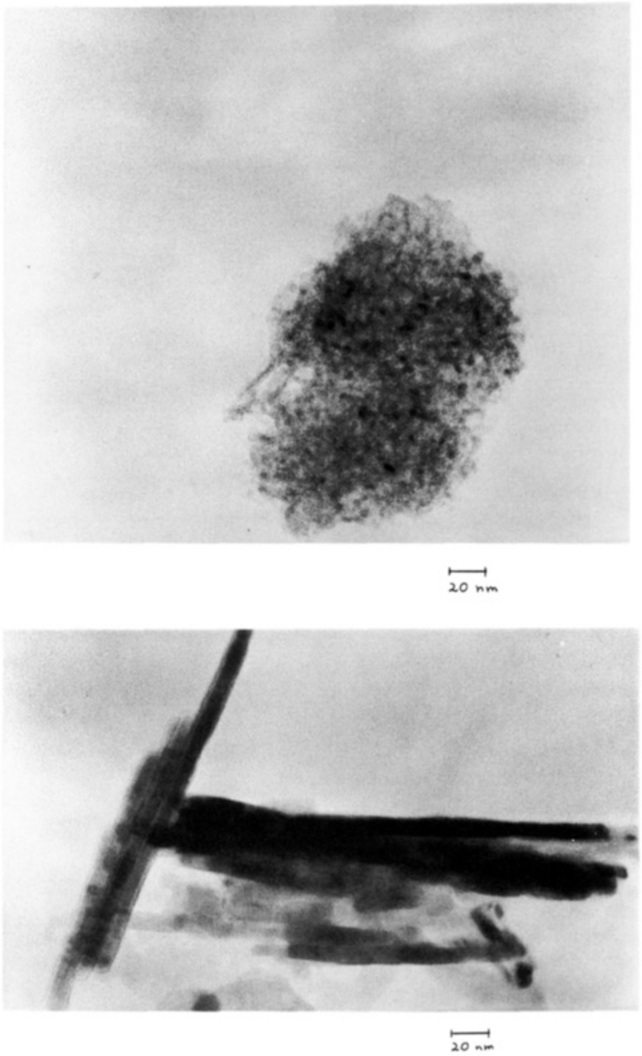

Figure 5. Transmission electron micrographs of (A) AP-MgO and (B) CP-MgO.

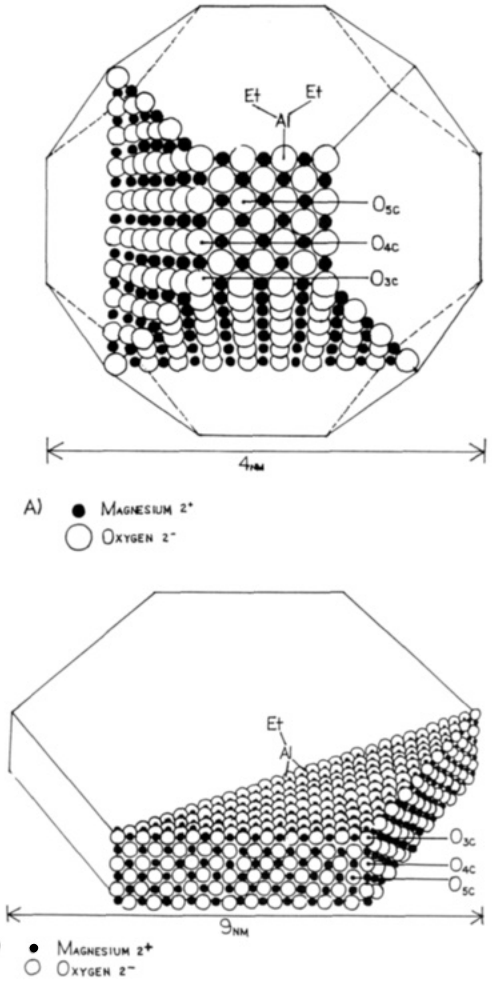

Figure 6. Idealized illustration of (A) AP-MgO and (B) CP-MgO average crystallites.

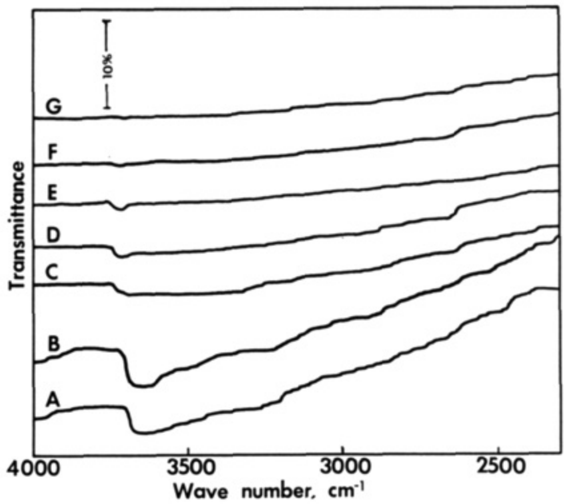

Figure 7. IR Spectra of CP-MgO heat treated/evacuated at various temperatures: (A) 120 °C; (B) 200 °C; (C) 300 °C; (D) 400 °C; (E) 500 °C; (F) 600 °C; (G) 700 °C.

$(OCH_3)_2$ precursor. The AP-MgO preparation is as follows:

$$Mg(OCH_3)_2 + 2H_2O \xrightarrow[\text{solvents}]{\text{organic}} Mg(OH)_2 + 2CH_3OH$$

$$\underset{\text{gel}}{Mg(OH)_2} \xrightarrow[265\ ^\circ C]{\text{autoclave}} \xrightarrow[\text{solvent}]{\text{vent}} \underset{\substack{\text{powder with some}\\ \text{residual } OCH_3}}{Mg(OH)_2}$$

By transmission infrared studies some striking differences were found between CP and AP samples, providing evidence that some $Mg-OCH_3$ groups did persist. Figure 7 shows the IR of CP-MgO after heat treatment at 120–700 °C. Note the presence of ν_{O-H} as a broad band that is decreased with progressively higher temperature treatments. So as expected, even after conversion to MgO, some surface –OH groups remained, and their concentration decreased with higher temperature treatments. Infrared studies of the AP samples showed quite a different picture. Figure 8 demonstrates the presence of OCH_3 groups; note the ν_{C-H} bands centered at 2800 cm^{-1}. Also note the broad ν_{O-H} bands that sharpen with progressively higher heat treatments. The most striking finding is that *OCH_3 groups persist even up to 400 °C, but upon heating to 500 °C they are completely eliminated.* According to mass spectral analysis (MS), thermal elimination causes the release of volatile products, mainly CO and, presumably, H_2:

$$Mg(OH)_2(OCH_3)_x \xrightarrow[\text{unbalanced equation}]{\text{heat}} MgO + H_2O + CO + H_2 + CO_2$$

(E) Hydroxyl Content. The number of surface –OH groups was determined by reaction with $AlEt_3$ in Decalin

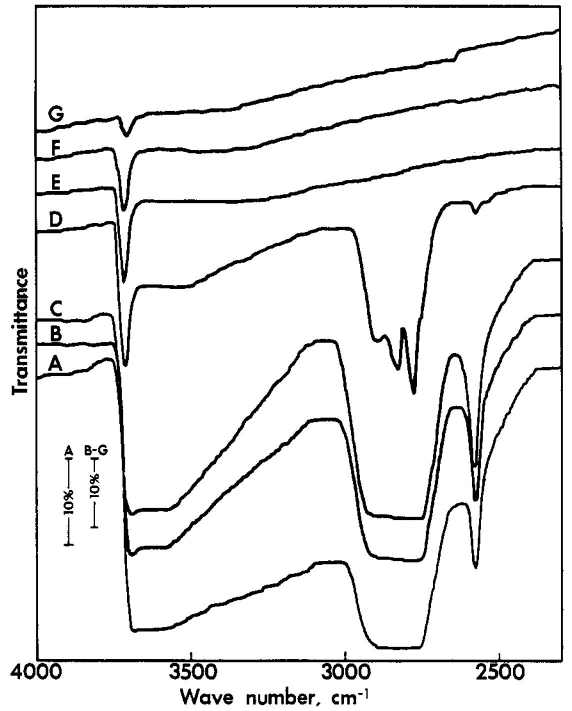

Figure 8. IR spectra of AP-MgO- heat treated/evacuated at various temperatures: (A) 120 °C; (B) 200 °C; (C) 300 °C; (D) 400 °C; (E) 500 °C; (F) 600 °C; (G) 700 °C.

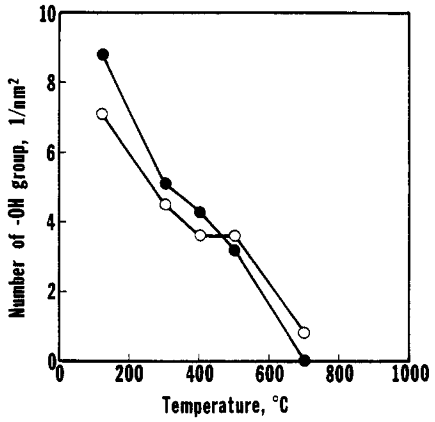

Figure 9. Number of surface hydroxyl group on AP-MgO- (○) and CP-MgO- (●) at various temperatures.

which is a modification of the procedure first reported by Sato and co-workers:[32]

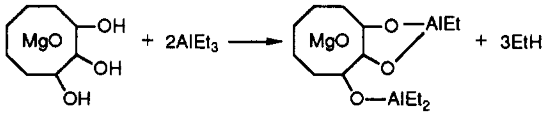

Note from Figure 9 that for both samples the surface hydroxyl group concentration decreased progressively with heat treatment temperature. Below 500 °C the CP-MgO contained a higher surface concentration than the AP-MgO sample, but this was reversed at higher temperature. This probably is a reflection of the presence of $-OCH_3$ groups in place of $-OH$ groups at lower temperatures in the AP-MgO sample.

It was possible to differentiate between the reaction of $AlEt_3$ with a single $-OH$ group or with two adjacent $-OH$ groups (linear vs bridged). This was done by first determining the total $-OH$ groups by pressure–volume measurements of EtH evolved. In a second experiment with a fresh MgO sample, about 0.5 equiv of $AlEt_3$ necessary to react with all the $-OH$ groups was added, and EtH evolved was measured. Then an excess of amyl alcohol was added and the additional EtH measured. Assuming that no tridentate adsorption took place, the fraction of linear vs bridged was determined as follows:

$$3N = E_1 + E_2$$

$$E_1 = n_L + 2n_B$$

$$E_2 = 2n_L + n_B$$

where N = moles of $AlEt_3$ chemisorbed, E_1 = moles evolved ethane during and after $AlEt_3$ adsorption, E_2 = moles evolved ethane during and after amyl alcohol addition, n_L = moles of $AlEt_3$ chemisorbed in a linear fashion, and n_B = moles of $AlEt_3$ chemisorbed in a bridged fashion.

The values of N, E_1, and E_2 are determined by experiment, so we can solve for n_L and n_B. The n_B/n_L ratios for AP samples treated at 300 and 500 °C, respectively, were 0.20 ± 0.03 and 0.05 ± 0.02; for CP samples these values were 0.95 ± 0.05 and 0.22 ± 0.03. As might be expected, this ratio decreased substantially for the CP-MgO heat treated at 500 °C, since the $-OH$ groups remaining would tend to be more isolated. Interestingly, this ratio changed much less with the AP-MgO sample. We suppose that this smaller change is due to the fact that at 300 °C, some surface $-OCH_3$ groups are still present on the AP-MgO sample which would tend to isolate the $-OH$ groups present. After 500 °C treatment, no $-OCH_3$ groups remain. Note that in this case the n_B/n_L ratio is significantly lower for the AP-MgO sample, and this cannot be explained by the prior presence of $-OCH_3$.[33]

(II) Adsorption Studies. (*A*) *Amounts of Pyridine Adsorbed.* Table I shows quantitative data for pyridine adsorption (using the spring balance method). The results are an average of several determinations. Note that the CP-MgO sample adsorbs slightly more pyridine/nm^2. (Note that the pretreatment temperature caused elimination of all $-OCH_3$ groups before room-temperature pyridine adsorption was studied.)

(*B*) *IR Studies of Adsorbed Pyridine.* Two techniques and three spectrometers were employed. First, FT-IR photoacoustic spectra were obtained. The AP and CP samples were heat treated under vacuum at 500 °C, and pyridine adsorbed at room temperature. Strong bands were observed at 1582, 1482, and 1439 cm^{-1} corresponding to ring vibration modes 8a, 19a, and 19b.[34] Two ν_{C-H} bands were also observed at 3087 and 3040 cm^{-1}. To remove physisorbed pyridine, the sample was evacuated cryogenically. Band intensities were reduced on CP-MgO, and

---

(33) On more careful examination of Figure 9, it can be seen that at lower preheat treatment temperatures, the number of surface $-OH$ groups is larger for CP-MgO, but at 500 °C a crossover occurs (the temperature where $-OCH_3$ loss takes place), and the AP-MgO then possess more surface $-OH$ species. We take this as evidence that can allow a rough determination of the number of surface $-OCH_3$ groups present. Thus, we can estimate that at pretreatment temperatures of 300 or 400 °C, about 10–15% of the total "OH sites" must be $-OCH_3$. This reasoning assumes that the intrinsic "need" of AP-MgO for surface-OH is close to but slightly higher than that for CP-MgO (as demonstrated by the higher pretreatment temperatures in Figure 9).

(34) These are ring vibrational modes. See: (a) Kline, C. H., Jr.; Turkevich, J. *J. Chem. Phys.* **1944**, *12*, 300. (b) Zerbi, G.; Crawford, B.; Overend, J. *J. Chem. Phys.* **1963**, *38*, 127. (c) Scokart, P. O.; Declerck, F. D.; Sempels, R. E.; Rouxhet, P. G. *J. Chem. Soc., Faraday 1* **1977**, 359. (d) Healey, M. H.; Wieser, L. F.; Arnett, E. M.; Wefers, K. *Langmuir* **1989**, *5*, 114.

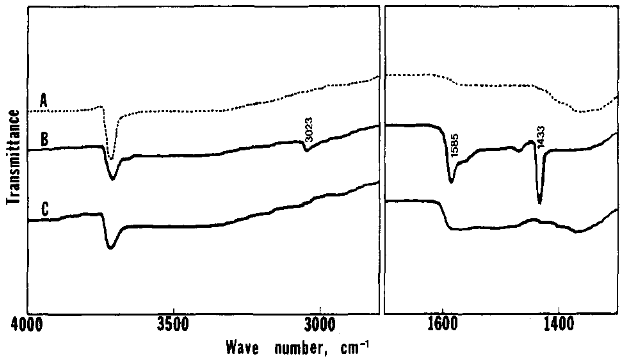

Figure 10. IR spectra of pyridine adsorbed on AP-MgO heat treated/evacuated at 500 °C. (A) background; (B) after evacuation at 25 °C for 40 min; (C) after evacuation at 100 °C.

Table II. FT-IR/PAS Bands for Adsorbed Nitrobenzene

	$\nu_{N\text{-}O(sym)}$ (±4 cm^{-1})	$\nu_{N\text{-}O(asym)}$ (±4 cm^{-1})
free nitrobenzene	1351 cm^{-1}	1527
on CP-MgO	1342	1518
on AP-MgO	1348	1524

broad bands due to modes 8a and 19b were observed at 1586 and 1439 cm^{-1}, and the ν_{C-H} bands were obviously perturbed. On AP-MgO with the same treatment, these bands were observed at 1593, 1439, and 1482 cm^{-1}. The resolution for the FT-photoacoustic spectrometer was ±4 cm^{-1}.

Transmission IR studies were carried out by pressing the CP-MgO and AP-MgO samples into 12- or 20-mm disks. After placing in an in situ IR cell,[35] they were heat treated at 500 °C for 2 h, cooled to room temperature, exposed to pyridine vapor, and then evacuated. Spectra were recorded on low-resolution and high-resolution instruments (±4 and ±1 cm^{-1}, respectively). Figure 10 shows the results for an AP-MgO sample. For the high-resolution experiments, the 8a and 19b modes were at 1596 ± 1 and 1442 ± 1 for both AP- and CP-MgO samples. These results are consistent with the LPy bonding mode. Furthermore, examination of Figure 10 shows that the MgO surface –OH groups *were not perturbed by pyridine adsorption*. Thus, surface –OH groups are apparently not involved in pyridine chemisorption. The pyridine must be binding to surface Mg^{2+} ion (the LPy mode).[34]

(*C*) *FT-IR/PAS Studies of Nitrobenzene Adsorption.* Nitrobenzene adsorption at its vapor pressure at room temperature caused a change in MgO color from white to deep yellow. The intensity of the color slowly increased with time. Upon manipulation of the sample in a glove bag the color faded to light yellow-brown. Equilibration with nitrobenzene proceeded for 2.5 h and a spectrum recorded, which showed bands at 1518 and 1342 cm^{-1} for CP-MgO and 1524 and 1348 cm^{-1} for AP-MgO (prior heat treatment of 500 °C; see Table II). Shifts to lower frequencies indicate more electron density.[36] Bands shifted more toward lower energy in the CP-MgO case, and these results indicate more basic (electron donating) character for the CP-MgO samples as compared to the AP-MgO samples.

(*D*) *Transmission IR Studies of Benzene and Xylene Adsorption.* As discussed above, pyridine adsorption occurred on the Mg^{2+} Lewis acid sites. Since adsorption of pyridine did not affect the surface –OH groups, it would be of interest to study other molecules that should adsorb on these Bronsted acid sites. Earlier work has shown that aromatic molecules such as benzene and xylene do absorb at Bronsted OH sites and that the magnitude of shift in this ν_{OH} band to lower frequency is a measure of Bronsted acidity.[37,38] Therefore, we have undertaken such studies for the AP- and CP-MgO samples.

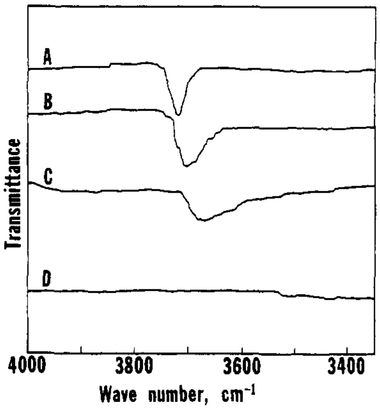

Figure 11. IR spectra of AP-MgO and CP-MgO in the presence of benzene vapor. (A) background AP-MgO without benzene; (B) AP-MgO; (C) CP-MgO; (D) benzene vapor.

Both benzene and xylene adsorption caused significant changes in the ν_{O-H} region, confirming the mode of adsorption expected (Figure 11). Repeated experiments using benzene or xylene always showed that the ν_{O-H} band broadened, more in the case of CP-MgO, and shifted further to lower energy. The shift for AP-MgO was always 15–25 cm^{-1} lower for benzene and 25–35 cm^{-1} for xylene, while for CP-MgO these shifts were 35–45 and 55–65 cm^{-1} for benzene and xylene, respectively. These differences are well outside experimental error (±4 cm^{-1}) and indicate that the CP-MgO possesses surface –OH groups of slightly greater acidity than AP-MgO.

Discussion

It would be expected that MgO crystallites would have a cubic morphology. Indeed, larger crystallites exhibit a cubic morphology, especially if prepared by burning Mg metal (MgO "smoke").[39] Other conventional preparations usually exhibit related morphologies, such as hexagonal flat particles.[9] In the present context, CP-MgO seems to be made up of a mixture of these shapes with definite crystal edges and planes. However, in the case of AP-MgO we have not been able to resolve any evidence of crystallinity in the electron microscope, although XRD patterns indicate the presence of very small crystallites. For purposes of illustration, we have drawn Figure 6 with a cubic internal structure but with the outer morphology octagonal, which mimics the spherodal appearance shown in the electron microscope. These tiny crystallites also appear to be quite uniform in size, but when forced to pack together form a powder with void areas such that a "pore" structure is developed. It should also be noted that this octagonal morphological representation requires a rather extensive edge structure where many 4-coordinate

---

[35] Matsuo, K.; Klabunde, K. J. *J. Org. Chem.* **1982**, *47*, 843.

[36] Roa, C. N. R. *Chemical Applications of Infrared Spectroscopy*; Academic Press: New York, 1963; Chapter IV, p 245.

[37] Hair, M. L.; Hertl, W. *J. Phys. Chem.* **1970**, *74*, 91.

[38] The strength of adsorption is related to the enthalpy of complex formation, as discussed by: Drago, R. S.; Vogel, G. C.; Needham, R. E. *J. Am. Chem. Soc.* **1971**, *93*, 6014.

[39] Morris, R. M.; Klabunde, K. J. *Inorg. Chem.* **1983**, *22*, 682.

ions would exist (O_{4c}^{2-} and Mg_{4c}^{2+}), whereas on flat surfaces five-coordination would predominate while on corners three-coordination would predominate.[7,40] Figure 6A represents AP-MgO crystallites that have been heat treated at 500 °C under vacuum. Overall, this material has a surface area of 348 m^2/g and average crystal diameter of 4.2 nm and would possess about 9000 total ions (Mg^{2+} plus O^{2-}). According to our measurements these crystallites possess 3.6 surface –OH groups/nm^2.

Also shown in Figure 6 is a realistic representation of a CP-MgO crystallite, according to the morphology observed in the electron microscope.[9] The surface –OH content is 3.5/nm^2. Note that this larger crystallite would exhibit considerably fewer edge sites. Thus, the ratio of O_{4c}^{2-}/O_{5c}^{2-} would be higher for the AP-MgO sample than the CP-MgO sample.

It may be a reasonable assumption that surface –OH groups would tend to concentrate on the lower coordinate edge and corner sites since these would be the more active sites and in need of further coordination. Thus, it would be expected that on average the AP-MgO would possess more edge- and corner-bound protons, with the understanding that vacancies of O^{2-} would exist on or in the crystallite in order to compensate the overall particle charge.

Now since the AP- and CP-MgO samples possess about the same number of surface –OH groups/nm^2, this picture would also require that more protons would be on plane sites on CP-MgO. Perhaps it is these sites that can more readily react with $AlEt_3$ to form bridged $EtAl(O)_2$ species. Thus, to explain our experimental results, we propose that surface –OH groups on flat planes can more readily shift to form geminal OH–OH sites that then react with $AlEt_3$. This is why the CP-MgO crystallites react to yield more bridged $EtAl(O)_2$ species.

This reasoning can be extended in order to rationalize the lower Bronsted acidity of surface –OH groups on AP-MgO. That is, edge bound protons should be less acidic since they would be bound more tightly to an O^{2-} of lower coordination and thus higher basicity.

Finally, we must try to rationalize why nitrobenzene accepts more electron density from the larger crystallites (CP-MgO) than the smaller ones (AP-MgO). Since nitrobenzene is believed to lie flat on the surface of MgO,[41] it would seem reasonable that the CP-MgO would offer more possibilities for this based on geometry. In addition, earlier work has suggested that base strength/electron-donor properties of MgO depends on long-range effects or essentially on the presence of electron-rich domains.[42] If a flat surface and multiple surface ions are necessary for more effective electron density transfer to nitrobenzene, the CP-MgO crystallites should be more effective compared with AP-MgO, and this is what is observed experimentally. The point might also be added that since it appears that CP-MgO is more capable of yielding more geminal surface –OH groups, this would require that other parts of the crystallite would be devoid of surface –OH. Perhaps this phenomenon also allows more access to OH free regions of the crystallite for nitrobenzene adsorption.

Pyridine adsorption also adds some interesting points. The IR studies revealed that adsorption took place at Lewis acid Mg^{2+} sites (the LPy mode). Also, the ν_{O-H} band was not perturbed at all. If it is assumed that pyridine does not adsorb at or adjacent to –OH groups and adsorbs in an end-on mode, we would expect that CP-MgO could adsorb more pyridine than AP-MgO because of the –OH pooling effect. In other words, if islands of –OH groups in close proximity can form more readily on CP-MgO, then more open areas would necessarily be available for pyridine adsorption to Mg^{2+} surface ions. Thus, the somewhat higher capacity of CP-MgO for pyridine adsorption can be rationalized.

Finally, a few comments about surface coverage can be made. For the AP-MgO and CP-MgO heat treated at 500 °C, the $AlEt_3$ experiments show that 30% of surface O^{2-} bear a proton. There must be a sufficient number of anion vacancies to accommodate this many protons, or about 15% if all were on the surface (which is not likely). For pyridine, the coverage of Mg^{2+} ions available on the surface is about 4% for AP-MgO and 6% for CP-MgO.

Although the differences are subtle, our results show that surface chemistry can be intrinsically different simply due to particle size and shape. Our rationale for these findings has been based mainly on shape/morphological arguments. And since smaller particles spontaneously take on a different morphology than larger ones, the question as to whether different sized particles with the same morphology would exhibit different surface chemistry cannot be answered at this time.

Acknowledgment. The support of the Army Research Office is acknowledged with gratitude.

---

(40) Colluccia, S.; Tench, A. J. *Proc. 7th Int. Congr. Catal., Tokyo* **1980**, 160.

(41) Klabunde, K. J.; Kaba, R. A.; Morris, R. M. *Inorg. Chem.* **1979**, *17*, 2684.

(42) Klabunde, K. J.; Matsuhashi, H. *J. Am. Chem. Soc.* **1987**, *109*, 1111.